Journal of Materials and Electronic Devices 2 (2025) 42-48

JOURNAL OF MATERIALS AND ELECTRONIC DEVICES
JMED

# Dielectric Characteristics of Bi doped ZnO Thin Film in Al/(Bi:ZnO)/p-Si/Au (MIS) Structures

Özkan GÖÇGELDİ[1], Çiğdem Şükriye GÜÇLÜ[2], Mümin Mehmet KOÇ[3,4], Burhan COŞKUN*[1]

[1]Kırklareli University, Faculty of Art and Science, Department of Physics, Kırklareli, Türkiye
[2]Gazi University, Faculty of Sciences, Department of Physics, 06500, Ankara, Türkiye
[3]Kırklareli University, School of Medical Service, Department of Medical Service and Techniques, Kırklareli, Türkiye
[4]Advanced Technologies Application and Research Center (ITUAM), Kırklareli University, Kırklareli, Türkiye

Thin films are fundamentals of modern electronic and optoelectronic devices and modern technologies. Various characterization techniques are proposed to characterize electrical and dielectric properties of thin films. These techniques are essential techniques to understand and illustrate the intrinsic characteristics of multi-layered structures and thin films. To be able to produce materials with advanced characteristics it is important to know and characterize such characteristics. Metal-insulator semiconductors (MIS) structures can be applied many optic and optoelectronic applications such as solar cells, photodiodes, photodetectors, etc. In the production process of such materials, doping or co-deposition is one of the most favourable methods. In this work, Zn thin films were doped with Bi at a rate of 5 %. As result product, Al/(Bi:ZnO)/p-Si/Au (MIS) type structures or Schottky diodes (SDs) were produced. In the previous works of our group investigated various electrical properties of MIS structures. In this work, ε'-V (real), ε''-V (imaginary) parts of dielectric characteristics, C-V, G/ω-V, and Cole/Cole plots, and electric modulus were investigated. Frequency related dielectric characteristics were assessed. Using such data, intrinsic characteristics of Al/(Bi:ZnO)/p-Si/Au SDs were evaluated. The obtained value of ε' (~9) even at 10kHz is considerable higher than the maximum value of traditional $SiO_2$, so they can more storage electrons or energy.

***Keywords:*** *MIS type structures with (Bi:ZnO) thin film; Dielectric characteristics; Impedance measurements and Nyquist curves; Complex electric modulus*

*Submission Date: 18 September 2025*
*Acceptance Date: 27 November 2025*

**Corresponding author: burhan.coskun@klu.edu.tr*

## 1. Introduction

Nanomaterials are superior structures built in 0D, 1D and 2D [1]. Each form provides various advantages and disadvantages. Quantum dots are often considered as 0D nanostructures while nanoparticles are considered as 1D nanostructures [1]. In this regard, thin films in nanoform were regarded as 2D structures. Thin films are essential tools of nanotechnology which are built by nanomaterials. In this regard, it is necessary to prepare efficient devices with good electrical and dielectric characteristics [2].

Different types of materials were proposed for this purpose such as metals, transition metals, organic molecules, rare earth elements, carbon-based molecules. Metal-insulator-semiconductor devices attracts the attention of researchers from various fields [3], [4], [5], [6]. Various types of metals were preferred in the production of MIS structures. Zn is one of the most favourable materials in optoelectronic applications [5], [7], [8], [9]. Zn thin films exhibit n type characteristics with band gap energy around 3.37 eV. Zn is quite stable and has high exciton binding energy. Zn is vastly found in nature. Zn thin films exhibit good optic transparency which make them a suitable candidate for optoelectronic applications. To alter and/or enhance the essential and intrinsic properties they are often combined with different materials. Such combination can be in different forms such as co-deposition, doping, producing alloys, etc. Various materials were used to dope Zn and ZnO based thin films such as Al, Ti, Cu, Co, Fe, etc. [5], [7], [8], [9], [10], [11], [12]. Doping materials using such materials enable them to enhance their optoelectronic, magnetic, electrical and dielectric properties. Among metals, Bi provide many advantages. Bi based materials often considered as photoactive materials. Therefore, they were used photocatalysis applications. They are also preferred in photothermal applications such as photothermal therapy, photothermal conversion applications as photothermal agents [13], [14], [15]. Bi has high atomic number. Therefore, they have high X-ray attenuation characteristics and utilized in X-ray applications. Bi also has large atomic structure, Therefore, doping any material with Bi may alter the intrinsic structures of the materials such as electrical, optical, optoelectronic and dielectric characteristics [16]. Because such large atoms alter the charge carrier and transfer mechanism, charge concentrations, free electron concentration, number of free atoms in conduction and valance band. Therefore, Bi has been used in photonic devices such as photodetectors, photodiodes and solar harvesting devices. For example, Khusayfan produced graphene oxide: Bismuth composite hybrid photodiodes [17]. Arumugam et al produced one dimensional $Zn:Bi_2S_3$ nanodevices for optoelectronic applications [18]. Demirezen et al. produce Bi doped PVA for photodiodes for room temperature applications [19]. Lavanya et al investigated Bi dopant effect on ZnO based photodetectors [20]. Huang et al. enhance the performance of Sn based photodiodes by Bi doping [21]. Sellan et al. produced CsPbBr3 perovskite single crystals for X-ray and gamma-ray sensing applications and used Bi as dopant [22]. In this study, we produced Bi doped ZnO films in Al/(Bi:ZnO)/p-Si/Au MIS structure. We assessed the dielectric characteristics of in Al/(Bi:ZnO)/p-Si/Au MIS structures. $\varepsilon'$-V (real), $\varepsilon''$-V (imaginary) parts of dielectric characteristics, $G/\omega$-V and Cole/Cole plots, and electric modulus were investigated. Frequency related dielectric characteristics were investigated.

## 2. Materials & Methods

### 2.1 Preparation of MIS diodes

Al/(Bi:ZnO)/p-Si/Au (MIS) structures were fabricated. In the fabrication process p-Si wafers were used as substrate. The substrate thickness is determined as 300 μm from the interfacial layer capacitance. The substrate was found to be in (100) orientations. The resistivity of substrate was found between 1-10 Ω.cm. A standard cleaning procedure was applied to the wafers [23]. Following the cleaning process, substrates were sonicated. Distilled water was used in sonicated process which took 10 mins. Wafers were dried under nitrogen gas. Then, clean substrates were transferred to a coating system which works under high vacuum. In this system, Au contacts were vapor-deposited on one side of the wafer under 1 mTorr. The thickness of Au contacts found as 150 nm. Following Au coating, the Au coated wafers were kept in 500 $C^0$ for 5 mins. A 0,1 M zinc acetate ($Zn\ (CH_3COO)_2$) and 0,1 M bismuth chloride ($BiCl_2$) solution were prepared in 15 mL of methoxy ethanol. In a separate beaker, 65 ml of NaOH was dissolved in methanol to prepare 0,4 M solution. To synthesize ZnO and Bi-doped ZnO, the 0.1 M zinc solution and the 0.4 M base solution were mixed. A %0,5 Bi:ZnO solution was grown on p-Si wafers using hydrothermal synthesis. Solution was dried at 50 °C for 1h. Lastly, an Al contact with a thickness of 150 nm and a diameter of 1 mm was deposited onto the Bi:ZnO films. Evaporation method was used in the production of contacts. An XTM (crystal thickness monitor) was used to determine the thickness of Al coating which were used as contacts.

### 2.2 Measurements

To complete the electrical characterization, silver wires were used to connect the device with the measurement system, which was positioned on a copper holder. To minimize the external effects dielectric measurements are conducted under vacuum conditions at 1 x $10^{-3}$ Torr using a Fytronix-FY-7000 characterization system. An image of Fytronix characterization system were presented in Figure 1. All the devices used for characterization and data collection were provided by Fytronix Co.

**Figure 1:** Image of Fytronix-FY-7000 characterization system used in the production of Al/(Bi:ZnO)/p-Si/Au (MIS) structures

## 3. Results and Discussions

In our previous work electrical characteristics of the diodes were investigated. In this work, dielectric characteristics were investigated. To assess such characteristic's following formula was used

$$\varepsilon^*(\omega) = \varepsilon'(\omega) - j\varepsilon'' \qquad (1)$$

$$\varepsilon^*(\omega) = \left(\frac{C_m d_i}{A\varepsilon_0}\right) - j\left(\frac{G_m d_i}{\omega A\varepsilon_0}\right) = \frac{C_m}{C_0} - j\frac{G_m}{\omega C_0} \qquad (2)$$

In eq 1, $\frac{\varepsilon_0 A}{d_i}$ represents capacitance of an empty capacitor ($C_0$), $\varepsilon_0$ (=8,85x$10^{-14}$ F/cm) is dielectric constant of free space, $d_i$ is the thickness of the interfacial layer or film, ω is angular frequency (=2πf). $C_m$ and $G_m/\omega$ are measured capacitance and conductance values, respectively. Figure 2 represents ε'-V values in 10kHz and 1MHz. Figure 3 represents ε''-V values in 10kHz and 1MHz. Figure 4 represents tanδ-V values obtained in 10kHz and 1MHz.

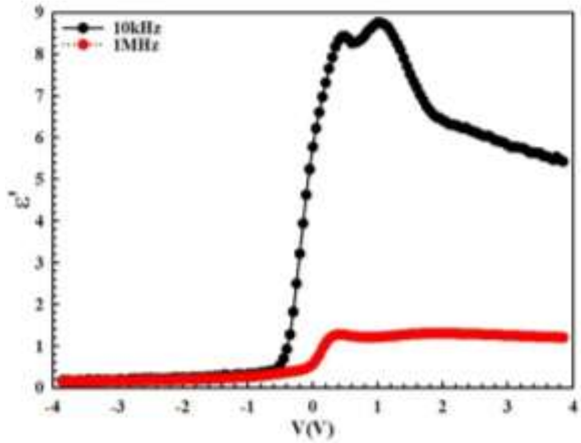


**Figure 2:** ε' vs V plots of the Al/(Bi:ZnO)/p-Si/Au (MIS) structure for 10kHz and 1MHz.

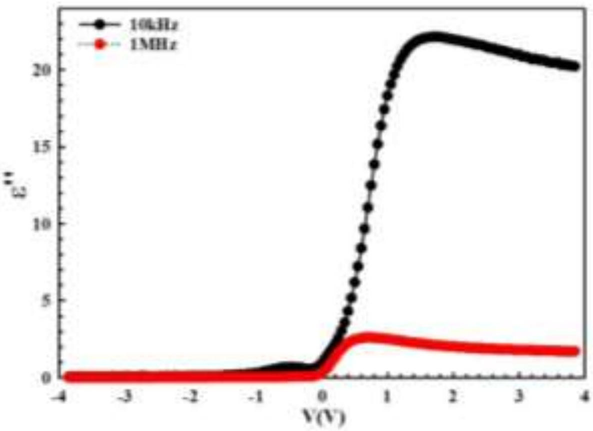


**Figure 3:** ε'' vs V plots of Bi doped ZnO thin film MIS structures obtained for 10kHz and 1MHz.

Real (ε'-V) and imaginary (ε''-V) parts of dielectric characteristics were evidenced. Both real and imaginary plots exhibit similarities with C-V ve G/ω-V plots which was presented in our previous work. ε'-V and ε''-V plots exhibit three distinctive zones which were inversion zone between -4,0/0,0V, depletion zone ($0 \leq V \leq 1.5$ V) and accumulation zone ($V \geq 1,5$ V). Figure 1 and Figure 2 illustrated that both ε' and ε'' exhibited increasing trend with decreasing frequency in forward bias region. Charges exist in traps, depending on their lifetimes (τ) traped charges can cause a polarization. Trapped charge related contribution is lost in higher frequencies since the period (T=1/ω) becomes lower than τ [24], [25].

Tanδ – V plots were obtained for both 10 kHz and 1 MHz and presented in Figure 4. For each frequency value different peaks were observed. As seen in the figure, each frequency-based measurement represents distinctive peaks. However, peak height and peak position alter with alteration of frequency values. Such a characteristics are associated with interface states positioned between semiconductor and interlayers. Moreover, distribution of interface states, their lifetimes and Maxwell-Wanger polarisations. Furthermore, such interface states may be restructured and redistributed under an electrical field [26], [27].

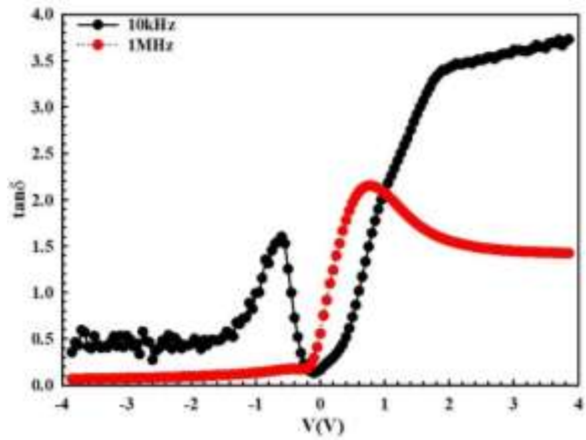


**Figure 4:** tanδ vs V plots of Bi doped ZnO thin film MIS structures obtained for 10kHz and 1MHz.

Figure 2, Figure 3, and Figure 4 demonstrate ε', ε'' and tanδ characteristics of Bi doped ZnO thin film MIS structures, respectively. Both accumulation and depletion zones exhibit strict frequency and potential related interface states characteristics.

Higher ε' and ε'' values are associated with thin interface layers, surface-dipole polarization and interface traps ($N_{ss}$) [27], [28]. When dipoles have enough time to adopt the frequency related alteration in electric field (T=1/2πf), ε', and ε'' values enhances [21], [22], [25], [26], [27], [28]. Moreover, enhanced relaxation time (τ ≫T), which enable localized charge migrations between traps, do not contribute ε' and ε'' values.

The Nyquist or (Cole-Cole) curves exhibit essential information about the nature of relaxation characteristics of interface states. Therefore, both the ε'' vs ε' and M'' vs M' curves have been drawn for 10 kHz and 1 MHz and represented in figures 5,6 and 9,10, respectively. As shown in these figures, while Cole-Cole curves have two semi arcs for 10 kHz, for 1 MHz it has only one semi arc. Such a case demonstrated that interface states lose the AC signal tracking ability by enhanced frequency. In another word, polarization was diminished and deviate from ideal Debye behaviour. Interface layers or dielectric modulus for dielectric materials do not

In interfacial layers or dielectric materials, electric modulus plots may not necessarily exhibit ideal circular or semicircular arc like behaviour; and they can exhibit asymmetrical characteristics. Smaller semi-circle observed at Cole-Cole curve for 10 kHz measurement exist as larger semi-circle for 1 MHz measurement. Such characteristics is an indication of enhanced polarization in the material [28].

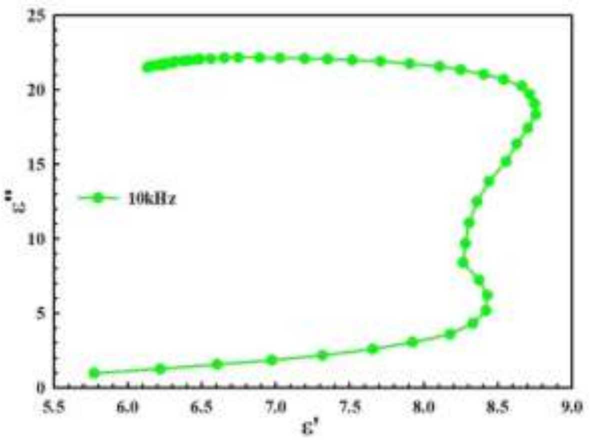


**Figure 5:** Cole-Cole (ε' vs ε'') curves of Bi doped ZnO thin film MIS structures obtained for 10 kHz

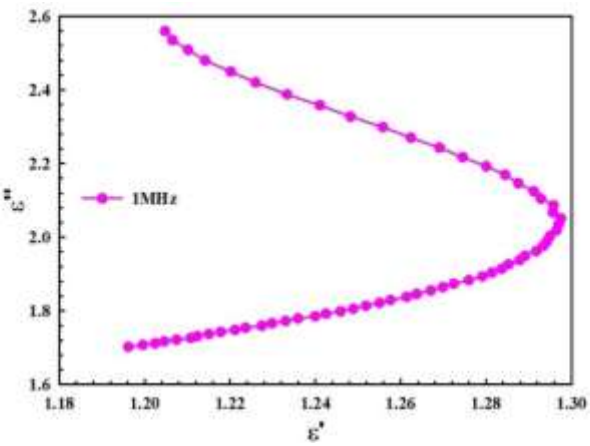


**Figure 6:** Cole-Cole (ε' vs ε'') curves of Bi doped ZnO thin film MIS structures obtained for 1 MHz

Real and imaginary formalism of complex dielectric modulus were defined as follows:

$$M^*(f) = \left(\frac{\varepsilon'}{\varepsilon'^2+\varepsilon''^2}\right) + j\left(\frac{\varepsilon''}{\varepsilon'^2+\varepsilon''^2}\right) \qquad (3)$$

Using the Eq (3) M' and M'' voltage related values obtained for 10 kHz and 1 MHz were presented in Figure 7 and Figure 8. These graphs are necessary to observe the effect of polarization and interface states and interface states for applied DC bias voltage for various potential upon dielectric characteristics and electric modulus. Voltage related M' and M'' plots were presented in Figure 7 and Figure 8. For both figures, dielectric loss enhances around 0 bias when ωτ=1. Such increases or peaks indicates charge carrier mobility from short distances to long distances. Moreover, increased frequency cause shifts in peak positions where apparent shifts toward forward bias zones were observed. Such shifts in the peak positions were originated from re-orientation and re-structuring process of electronic charges and dipoles [28].

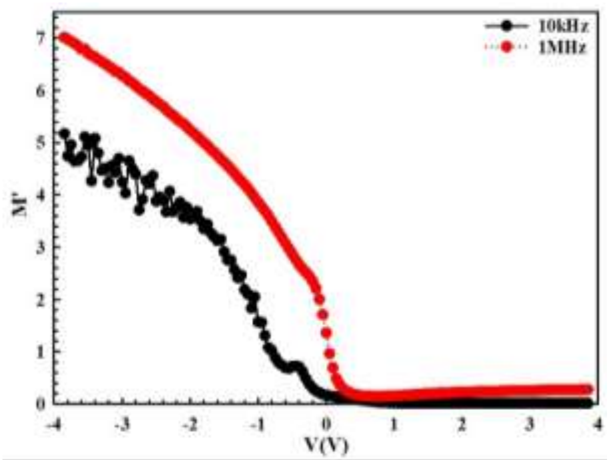


**Figure 7:** Real part of electrical modulus (M') vs V for Bi doped ZnO thin film MIS structures obtained for 10kHz and 1MHz.

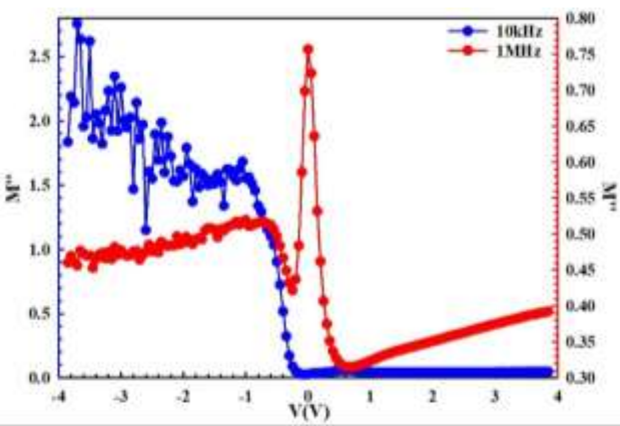


**Figure 8:** Imaginary part of electrical modulus (M'') vs V for Bi doped ZnO thin film MIS structures obtained for 10kHz and 1MHz.

Frequency and voltage related significant alteration occurring on both imaginary and real parts of M originates from localized charges, interface states, and dipoles. Such distribution occurs in low and mid-range frequencies and called as Maxwell-Wagner polarization (MWP) [28], [29], [30], [31], [32].

Decrease in M' and M'' values were observed while frequency is increased and results were presented in Figure 7 and Figure 8. Such characteristics is attributed to short range mobility of electronic charges.

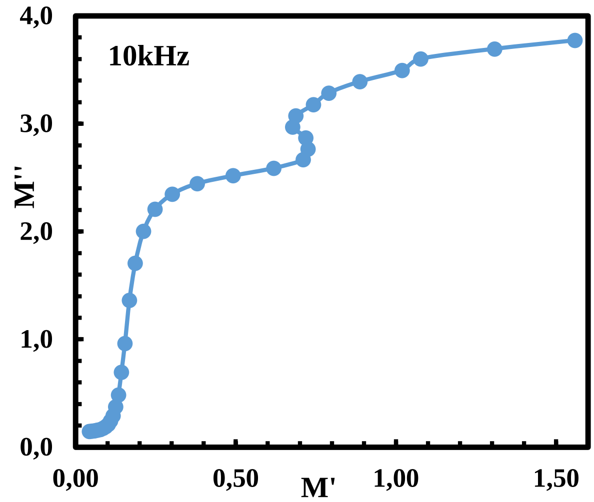


**Figure 9:** Cole-Cole (M' vs M'') curves of Bi doped ZnO thin film MIS structures obtained for 10 kHz

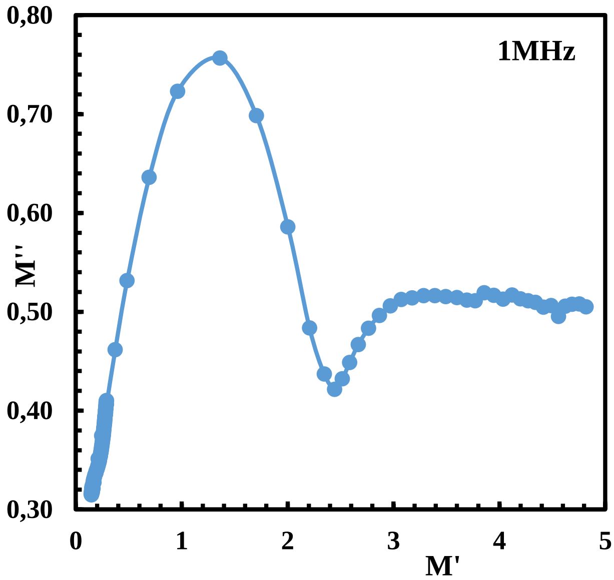


**Figure 10:** Cole-Cole (M' vs M'') curves of Bi doped ZnO thin film MIS structures obtained for 1 MHz

Frequency related alteration in ε* and M* values and their real and imaginary parts were originated from relaxation and interface state related effects. The observed double semi arcs in the ε'' vs ε' and M" vs M' curves for 10 kHz are the result of the grains and grain boundaries. Similar results were also reported in the literature in recent years [27-32].

## 6. Conclusion

A 0.5% Bi doped ZnO thin films in Al/(Bi:ZnO)/p-Si/Au structures were produced. Dielectric characteristics of Bi doped ZnO thin film structures were investigated in 10 kHz and 1 MHz under varying voltage. Various dielectric characteristics such as real and imaginary part of dielectric characteristics, real and dielectric characteristics of electrical modulus were investigated. All parameters were found to be related to frequency. It was found that interface states, polarizations, interlayer charge mobilities have essential contributions to dielectric characteristics of Bi doped ZnO thin film structures.

**Acknowledgements**

Part of this work was supported by Kırklareli University Scientific Research Coordination Office with project number KLUBAP 306. Part of this research was conducted using the facilities of Kırklareli University Advanced Technologies Application and Research Center (ITUAM).

## Author Contributions

Ö.G.: Conceptualization, writing, data acquisition
Ç.Ş:G: Conceptualization, data acquisition, calculation
M.M.K.: Editing, English check, writing
B.C.: Conceptualization, writing, supervising

## References

[1] Q. Wu, W. Miao, Y. Zhang, H. Gao, and D. Hui, “Mechanical properties of nanomaterials: A review,” *Nanotechnol Rev*, vol. 9, no. 1, pp. 259–273, Mar. 2020, doi: 10.1515/ntrev-2020-0021.

[2] P. S. Alexopoulos and T. C. O’Sullivan, “Mechanical Properties of Thin Films,” *Annual Review of Materials Science*, vol. 20, no. 1, pp. 391–420, Nov. 2003,

[3] Boris Polyakov, Alexei Kuzmin, Sergei Vlassov, Edgars Butanovs, Janis Zideluns, Jelena Butikova, Robert Kalendarev, Martins Zubkins, A comparative study of heterostructured $CuO/CuWO_4$ nanowires and thin films, Journal of Crystal Growth, 480, 2017, 78-84, doi:10.1146/ANNUREV.MS.20.080190.002135.

[4] K. R. Rajesh and C. S. Menon, “Electrical and optical properties of vacuum deposited MnPc thin films,” *The European Physical Journal B - Condensed Matter and Complex Systems 2005 47:2*, vol. 47, no. 2, pp. 171–176, Oct. 2005, doi: 10.1140/EPJB/E2005-00317-x.

[5] B. Coşkun, “Investigation of dielectric properties of Ag-doped ZnO thin films,” *J Mol Struct*, vol. 1209, p. 127970, Jun. 2020, doi: 10.1016/J.MOLSTRUC.2020.127970.

[6] M. İlhan, Z. Görünmez Güngör, M. M. Koç, B. Coşkun, and F. Yakuphanoğlu, “Infrared light sensing performance of CdO-doped $TiO_2$ thin films,” *Journal of Materials Science: Materials in Electronics*, vol. 34, no. 1, pp. 1–11, Jan. 2023, doi: 10.1007/S10854-022-09411-2/FIGURES/6.

[7] I. S. Yahia, G. F. Salem, J. Iqbal, & F. Yakuphanoğlu, “Linear and nonlinear optical discussions of nanostructured Zn-doped CdO thin films,” *Physica B Condens Matter*, vol. 511, pp. 54–60, Apr. 2017, doi: 10.1016/J.PHYSB.2017.01.030.

[8] B. Coşkun &M. M. Koç, “Dielectric Characterization of ZnO: $TiO_2$ Nanocomposites,” *JOURNAL OF MATERIALS AND ELECTRONIC DEVICES*, vol. 3, no. 1, pp. 30–33, Aug. 2021, Accessed: Apr. 03, 2022. [Online]. Available: http://dergi-fytronix.com/index.php/jmed/article/view/177

[9] E. Karakuş, Ç. Ş. Güçlü, M. M. Koç, and B. Coşkun, “Current–Voltage Characteristics of Al/(CdO:ZnO:NiO:Ti)/p-Si/Al Quaternary Functional Schottky Diodes,” *Journal of Materials and Electronic Devices*, vol. 4, no. 1, pp. 36–45, Nov. 2024, Accessed: Sep. 21, 2025. [Online]. Available: http://dergi-fytronix.com/index.php/jmed/article/view/306

[10] B. Coşkun *et al.*, “Optoelectrical properties of Al/p-Si/Fe:N doped ZnO/Al diodes,” *Thin Solid Films*, vol. 653, pp. 236–248, May 2018, doi: 10.1016/j.tsf.2018.03.033.

[11] N. Aslan, “Synthesis and Characterization of ZnO@Fe3O4 Composite Nanostructures by Using Hydrothermal Synthesis Method,” *Turkish Journal of Nature and Science*, vol. 11, no. 1, pp. 95–101, Mar. 2022, doi: 10.46810/TDFD.1011220.

[12] M. Koç *et al.*, “Electrical characterization of solar sensitive zinc oxide doped-amorphous carbon photodiode,” *Optik (Stuttg)*, vol. 178, pp. 316–326, 2019, doi: https://doi.org/10.1016/j.ijleo.2018.10.008.

[13] M. M. Koç, U. Paksu, N. K. Yetim, B. C. Coşkun, E. Hasanoğlu Özkan, and M. Erkovan, “Nanoparticles in photothermal therapy-based medical and theranostic applications: an extensive review,” *The European Physical Journal Plus 2025 140:6*, vol. 140, no. 6, pp. 1–54, Jun. 2025, doi: 10.1140/EPJP/S13360-025-06452-4.

[14] M. M. Koç, N. Aslan, A. P. Kao, and A. H. Barber, “Evaluation of X-Ray tomography contrast agents: A review of production, protocols, and biological applications,” *Microsc Res Tech*, vol. 82, no. 6, pp. 812–848, Jun. 2019, doi: 10.1002/jemt.23225.

[15] N. Aslan, B. Ceylan, M. M. Koç, and F. Findik, “Metallic nanoparticles as X-Ray computed tomography (CT) contrast agents: A review,” *J Mol Struct*, vol. 1219, p. 128599, Nov. 2020, doi: 10.1016/j.molstruc.2020.128599.

[16] Y. Xu *et al.*, “Bismuth-doping induced red-shifted spectral response of homo-epitaxial $MAPbBr_3$ photodiodes,” *APL Mater*, vol. 11, no. 12, Dec. 2023, doi: 10.1063/5.0180460.

[17] N. M. Khusayfan, “Coumarin:GO doped $Bi_2O_3$ composites/p-type silicon hybrid photodiodes,” *Synth Met*, vol. 222, pp. 299–308, Dec. 2016, doi: 10.1016/j.synthmet.2016.11.003.

[18] J. Arumugam *et al.*, “Fabrication of one-dimensional Zn-doped $Bi_2S_3$ nanorods for photodiode applications,” *Luminescence*, vol. 39, no. 9, Sep. 2024, doi: 10.1002/bio.4901.

[19] S. Demirezen, Ş. Altındal, and İ. Uslu, “Two diodes model and illumination effect on the forward and reverse bias I–V and C–V characteristics of Au/PVA (Bi-doped)/n-Si photodiode at room temperature,” *Current Applied Physics*, vol. 13, no. 1, pp. 53–59, Jan. 2013, doi: 10.1016/j.cap.2012.06.009.

[20] S. Lavanya *et al.*, “Effect of Bi doping on the opto-electronic properties of ZnO nanoparticles for photodetector applications,” *J Photochem Photobiol A Chem*, vol. 446, p. 115119, Jan. 2024, doi: 10.1016/j.jphotochem.2023.115119.

[21] Y. Huang *et al.*, “Boosting the performance of self-powered SnO2-based UV photodetectors via Bi doping modulation for UV imaging and optical communication,” *Nano Materials Science*, May 2025, doi: 10.1016/j.nanoms.2025.03.008.

[22] P. Sellan *et al.*, “Preparation of bismuth-doped CsPbBr3 perovskite single crystals for X-ray and gamma-ray sensing applications,” *Mater Adv*, vol. 5, no. 15, pp. 6309–6318, 2024, doi: 10.1039/D4MA00455H.

[23] S. Özden & M. M. Koç, “Wet-chemical etching of GaAs(211)B wafers for controlling the surface properties,” *International Journal of Surface Science and Engineering*, vol. 13, p. 79, 2019, doi: 10.1504/IJSURFSE.2019.102359.

[24] K. Prabakar, Sa. K. Narayandass, and D. Mangalaraj, “Dielectric properties of Cd0.6Zn0.4Te thin films,” *physica status solidi (a)*, vol. 199, no. 3, pp. 507–514, Oct. 2003, doi: 10.1002/pssa.200306628.

[25] A. A. Sattar and S. A. Rahman, “Dielectric Properties of Rare Earth Substituted Cu–Zn Ferrites,” *physica status solidi (a)*, vol. 200, no. 2, pp. 415–422, Dec. 2003, doi: 10.1002/pssa.200306663.

[26] S. Tewari, A. Bhattacharjee, and P. P. Sahay, “Structural, dielectric, and electrical studies on thermally evaporated CdTe thin films,” *J Mater Sci*, vol. 44, no. 2, pp. 534–540, Jan. 2009, doi: 10.1007/s10853-008-3088-x.

[27] Bibin John & S. Varadharajaperumal, “Comprehensive Review on CdTe Crystals: Growth, Properties, and Photovoltaic Application,” *Physics of Metals and Metallography*, vol. 124, no. 14, pp. 1795–1812, Dec. 2023, doi: 10.1134/S0031918X2110094X.

[28] Ç. Ş. Güçlü, Ş. Altındal, M. Ulusoy, and A. E. Tezcan, "The study of the dependence of dielectric properties, electric modulus, and ac conductivity on the frequency and voltage in the Au/(CdTe:PVA)/n-Si (MPS) structures," *Journal of Materials Science: Materials in Electronics*, vol. 35, no. 18, p. 1225, Jun. 2024, doi: 10.1007/s10854-024-12921-w.

[29] Ç. Ş. Güçlü, Ş. Altındal, & E. Erbilen Tanrikulu, "Voltage and frequency reliant interface traps and their lifetimes of the MPS structures interlayered with CdTe:PVA via the admittance method," *Physica B Condens Matter*, vol. 677, p. 415703, Mar. 2024, doi: 10.1016/j.physb.2024.415703.

[30] G. Fussell, J. Thomas, J. Scanlon, A. Lowman, and M. Marcolongo, "The effect of protein-free versus protein-containing medium on the mechanical properties and uptake of ions of PVA/PVP hydrogels," *J Biomater Sci Polym Ed*, vol. 16, no. 4, pp. 489–503, Jan. 2005, doi: 10.1163/1568562053700219.

[31] A. Ashery, M. A. Moussa, and G. M. Turky, "Enhancement of Electrical and Dielectric Properties of Graphene Oxide-nanoparticle Based Devices," *Silicon*, vol. 14, no. 5, pp. 1913–1924, Apr. 2022, doi: 10.1007/s12633-021-00943-6.

[32] G. Kandhol, H. Wadhwa, S. Chand, S. Mahendia, and S. Kumar, "Study of dielectric relaxation behavior of composites of Poly (vinyl alchohol) (PVA) and Reduced graphene oxide (RGO)," *Vacuum*, vol. 160, pp. 384–393, Feb. 2019, doi: 10.1016/j.vacuum.2018.11.051.